

Medical Engineering and Physics

Microarchitecture and morphology of bone tissue over a wide range of BV/TV assessed by micro-computed tomography and three different threshold backgrounds --Manuscript Draft--

Manuscript Number:	MEP-D-21-00592R1
Article Type:	Paper
Section/Category:	Regular Issue Paper
Keywords:	Bone; cancellous; Cortical; density; Porosity; BV/TV; Specific surface; μ CT
Corresponding Author:	Peter Zioupos, DSc, PhD, BSc Cranfield University Swindon, UNITED KINGDOM
First Author:	George J Adams, PhD, BSc
Order of Authors:	George J Adams, PhD, BSc Richard B Cook, PhD, BSc John Hutchinson, PhD, BSc Peter Zioupos, DSc, PhD, BSc
Abstract:	<p>The microarchitecture of bone both results from and in turn affects the remodelling process. Bone-specific surface, for instance, is one of these important microarchitectural parameters because remodelling is also considered to be a surface-mediated phenomenon (Berli et al. 2017). An understanding of these structural parameters across the widest possible range of porosity is essential to illuminating how bone reacts to disease, in different skeletal sites and in either its cancellous or cortical forms. 112 samples from an elephant femur were examined by micro-computed tomography (μCT), 31 of which contained both mineralised and demineralised tissue. A critical factor in all scans is setting the correct threshold (with background the surrounding medium) and hence 3 different backgrounds were used: air, water and collagen. The effect of the 3 background thresholds on the physical characteristics of bone (BS/TV, BS/BV, TbSp, TbTh, D mat, vs BV/TV) was then determined. The results showed that using a threshold set by the collagen background had a profound effect on the histomorphometry bone parameters when assessed by μCT. However, the differences between air and water were not significant, suggesting that comparable data can be produced in a laboratory environment when scanning porous bone samples under either wet or dry conditions-- counter to common belief. Determining which is more suitable, air or water, in laboratory and in clinical μCT imaging is important to improve the quality and relevance of biomechanics research. The data with collagen as the threshold were illuminating as they showed that remodelling rates and the relative organic to mineral presence varied with BV/TV, concurring with some other recent studies [2,3,4].</p>

Highlights

- Micro-CT scanning is a powerful non-destructive and non-invasive method to study inner structure of bone tissue.
- Setting the most appropriate scanning threshold is critical in producing accurate bone microarchitectural parameters by micro CT.
- Data produced with 3 typical backgrounds such as air, water and organic material can differ by as much as 85%.
- Overall the values produced by using organic material as threshold deviated greatly from those based on air and water.
- Air and water thresholds on the whole differed little which is important for scanning isolated specimens in lab work.

Microarchitecture and morphology of bone tissue over a wide range of BV/TV assessed by micro-computed tomography and three different threshold backgrounds

Adams GJ^a, Cook RB^b, Hutchinson JR^c, Zioupos P^{a*}

a Cranfield Forensic Institute, Cranfield University, Defence Academy of the UK, Shrivenham, UK

b nCATS, School of Engineering Science, University of Southampton, Southampton, UK

c Structure and Motion Laboratory, Department of Comparative Biomedical Sciences, The Royal Veterinary College, Hatfield, UK

Abstract

The microarchitecture of bone both results from and in turn affects the remodelling process. Bone-specific surface, for instance, is one of these important microarchitectural parameters because remodelling is also considered to be a surface-mediated phenomenon (Berli et al. 2017). An understanding of these structural parameters across the widest possible range of porosity is essential to illuminating how bone reacts to disease, in different skeletal sites and in either its cancellous or cortical forms. 112 samples from an elephant femur were examined by micro-computed tomography (μ CT), 31 of which contained both mineralised and demineralised tissue. A critical factor in all scans is setting the correct threshold (with background the surrounding medium) and hence 3 different backgrounds were used: air, water and collagen. The effect of the 3 background thresholds on the physical characteristics of bone (BS/TV, BS/BV, TbSp, TbTh, D_{mat} , vs BV/TV) was then determined. The results showed that using a threshold set by the collagen background had a profound effect on the histomorphometry bone parameters when assessed by μ CT. However, the differences between air and water were not significant, suggesting that comparable data can be produced in a laboratory environment when scanning porous bone samples under either wet or dry conditions-- counter to common belief. Determining which is more suitable, air or water, in laboratory and in clinical μ CT imaging is important to improve the quality and relevance of biomechanics research. The data with collagen as the threshold were illuminating as they showed that remodelling rates and the relative organic to mineral presence varied with BV/TV, concurring with some other recent studies [2,3,4].

Keywords: Bone; cancellous; Cortical; density; Porosity; BV/TV; Specific surface; μ CT

* Corresponding author: p.zioupos@cranfield.ac.uk

1. INTRODUCTION

Determination of the structural characteristics of bone is essential in understanding bone's mechanical properties, rates of remodelling, or adaptation, and its susceptibility to disease. We have recently published [1] a new computational paradigm to illustrate that the local mineralisation patterns in bone follow certain rules, whereby the mineral content (through a diffusion via the bone active surface area) depends on the depth from the surface and the amount of active surface that is available. This model explained in detail some fundamental observations [3] we published in 2008 in which bone material density varies with BV/TV (bone volume/total volume of bone). The plot of bone material density vs. apparent density showed a bifurcating curve shaped like a 'boomerang' [3] showing that bone has the highest material density values for the lowest (cancellous) and highest (cortical) BV/TV values. This behaviour which was produced with the Archimedes principle technique (submersion in fluid to produce material density values) was later on corroborated with another independent technique which was both non-invasive and non-destructive, namely the use of microCT scanning [4]. Micro-CT scanning is a powerful method which can both confirm the densities bifurcating curve and also produce microarchitectural parameters across the full range of porosities. Three of the most important features of bone structure are the porosity, specific surface, and density [3,5,6]. Porosity is the void volume per unit volume of bone, which is often expressed as its inverse BV/TV (bone volume/total volume). Specific surface (BS/TV) is the total internal surface area per unit volume of bone tissue [5]. Density can be considered in two ways. Firstly, as apparent density (D_{app}), this can be defined as the mass over the whole volume of the sample, and its nearest equivalent in scanning is the bone volume mineral density (BMD). Secondly, as material density (D_{mat}), which can be defined as the mass of the bone over the volume occupied by the material itself, with its nearest equivalent in scanning being the tissue mineral density (TMD). BV/TV is a dimensionless ratio, BS/TV has the units cm^{-1} , and both densities have the same units g/cm^3 . BV/TV and D_{mat} are important because bone's primary role within the body is as a structural material in both its cortical or cancellous (cellular) forms [7]. We have recently argued that an understanding of how D_{mat} varies with BV/TV is important in bone disease specifically when trying to understand the impact of osteoporosis [1-4]; and also important to understand the relationship between the other histomorphometry variables well and within 'normal' bone, so that irregularities in diseased bone can be identified [8-10].

One of the important histomorphometric parameters is active surface area because it is widely accepted that during the remodelling process, osteoclasts and osteoblasts act primarily through the

openly accessible active surface available within bone tissue [11]. This remodelling effect is surface-mediated either because the process is one where the cells have to be physically present and reach
35 a certain area, or where the metabolites need to diffuse across a boundary in and out of the bone tissue into the medium. The level of activity of the cells is hormonally and metabolically driven and is related to the total area over which the cells can act. As such the total BS/TV will impact on the resultant rate of bone remodelling at specific sites [12,13]. BS/TV is determined by the micro-architecture of bone including all places where there is a void, such as osteocyte lacunae, osteonal
40 canals and trabecular structure. Models of bone remodelling in the cortical regions of bone with variations in the specific surface have shown that with a higher specific surface the rate of remodelling is increased [14]. Better knowledge of the variations in specific surface for both cortical and cancellous regions can help in improving the quality and accuracy of computational modelling of bone remodelling which in turn can help with the understanding of bone condition in health or
45 disease. This was recently demonstrated using a computational approach to simulate the remodelling process of bone with a dependence on the surface area [1]. The relationship between the porosity and specific surface of bone has been previously investigated by Martin [5] in an invasive way by using a series of histological slices. However, this method is time-consuming and destructive so is not ideal in research and clearly impossible in clinical settings. The method also carries limitations in resolution and inherent error as it is limited by slice thickness. By using μ CT this
50 relationship can be examined more easily with a potentially higher accuracy [15]. μ CT can also access all internal structure by being 'optically' invasive throughout and that includes both open and closed cells. However, μ CT is not without its own limitations in the sense that the reproducibility of the results is critically dependent on the set-up parameters. One of these parameters is the
55 threshold background level, which can be the surrounding medium (air, water, fat) or even a certain degree of mineralisation starting from organic matrix with no mineral at all, the osteoid (collagen). Here we investigate bone microarchitectural parameters produced by μ CT across a very wide range of porosities and as a function of this porosity level. We postulate that a more fundamental knowledge of the inner workings of bone at the microarchitecture may result by understanding the
60 interplay between porosity and the other basic microarchitectural parameters and that can come by controlling more precisely the different scanning threshold level backgrounds which define where bone starts and where bone ends.

2. MATERIALS & METHODS

65 2.1 Specimens

In this study, samples were taken from the right femur of an adult Asian elephant (3432 kg, 24 years old). The advantage of using the femur of such a large mammal is that a large number of samples (n=112) over a wide range of BV/TVs (0.04-0.98) can be taken. The suitability of this tissue was confirmed in previous studies [3,16]. The specimen was collected shortly after the animal's
70 euthanasia (for reasons unrelated to this study) at ZSL Whipsnade Zoo (Bedfordshire, UK) and frozen (-20°C) until testing. The samples were cut in either cylindrical cores or cubes approximately 10mm³, larger than the minimum size recommended by [18]. Full preparation details can be found in our previous work [2,3,15]. In a subsection of samples (n=31) a 2mm thick slice was taken from the bottom of each sample and submerged in EDTA for 168hrs (7 days) with daily changes to fully
75 demineralise the slice. This demineralisation process left behind undamaged organic matrix (which is mostly collagen), which could then be used to provide a threshold for the organic bone material during μ CT scanning. The known density of this matrix was approximately 1.1 g/cm³ and this was confirmed with the Archimedes method similar to previous application [3]. All samples were stored frozen (-20°C) until testing and were allowed to defrost for 2hrs prior to imaging.

80 2.2 Imaging- μ CT

All samples were imaged using a cone beam μ CT scanner, Nikon XTEK XT H 225 (Nikon Metrology, Herts HP23 4JX, UK). The samples were imaged in ABS plastic sample holders at 50 kV, 65 μ A. The resultant voxel size was \sim 16 μ m, making them suitable to determine the samples' morphology with adequate resolution [17]. All 112 samples were imaged whilst fully submerged in deionised water.
85 The 31 samples were additionally imaged in air with both their mineralised volumes and the demineralised slices being present in the vials. All scans were manually reconstructed using CT Pro 3D. During reconstruction, conditions were optimised to reduce beam hardening.

Figure 1

90

The effect from using the three different backgrounds to produce grey level thresholds is shown in fig. 1. By using a different threshold, there is a virtual shift at the point where the perceived surface of the bone is. As the density of the background increases so does the threshold grey value which is placed halfway between the chosen peaks. As can be seen in the histograms of Fig. 1, there is

95 potentially a noticeable shift in the position of the 'bone' threshold for the three backgrounds
consisting of air, water and organic matrix (collagen).

2.3 Image Analysis

Image analysis was carried out using VGSTUDIO MAX 2.2. Regions of interest (ROI) were taken from
the centre of each sample $\sim 9 \text{ mm}^3$ to exclude any external surfaces from the scan. These surfaces,
100 which have been introduced during the sample preparation process, were excluded as the software
would consider them in the BS/TV calculations and therefore give erroneous results. A surface
determination was performed using the grey level of an internal void as the background and the
largest void-less section of bone, as per the manufacturers' recommendations. This thresholding
105 process introduces a surface threshold at an intermediate point between the average grey values of
these two sections. For the samples imaged with a collagen slice, the collagen was used as the
background. After the surface determination an automatic morphometric report was exported. This
contained: bone volume (BV/TV), specific surface (BS/TV), mean trabecular thickness (TbTh), mean
trabecular number (TbN), and mean trabecular spacing (TbS).

From the histogram the mean, mode, minimum and maximum grey level were recorded to be used
110 in calculation of the material density. A QRM-MicroCT-HA (QRM GmbH Dorfstrasse 4, 91096,
Moehrendorf, Germany) calibration phantom was imaged and reconstructed under the same
conditions in order to determine D_{mat} . Determination of material density is more favourable than
deriving Hounsfield (HU) units, which are typically used in medical CT imaging, as HU is an x-ray
specific expression of a materials linear attenuation coefficient and does not have any consistent
115 conversion to physical density measurements. Therefore, using material density enables for
comparison with physical density measurements that HU otherwise does not.

2.4 Density Calibration

Fig. 2 shows the histogram of the QRM HA calibration phantom alongside the 3D image of the scan,
both obtained using VGSTUDIO. Within VGSTUDIO, each density was isolated and the average grey
120 scale was determined and plotted against the density provided by the supplier. This provided a
calibration curve from which the density of the bone samples could be determined. The average
grey value of each sample was measured and using the calibration curve D_{mat} was determined
(Fig.2b).

125 **Table 1. Properties of QRM calibration phantom.**

Sample	Mean grey	Density (g/cm ³)	Mineral %
Standard 1	36.10	1.13	0
Standard 2	48.60	1.18	0.42
Standard 3	112.20	1.26	15.89
Standard 4	337.20	1.64	48.29
Standard 5	478.45	1.90	63.17

Figure 2

Figure 3

130 **3. RESULTS**

A statistical comparison of the three different thresholds is shown in Table 2. The results of the comparison showed that the air and water thresholds were not statistically different when comparing the two datasets. This suggests that imaging bone in air and in water using μ CT produced no significant difference across the full range of bone porosities. A comparison of the three
135 thresholds showed that increasing the value to the collagen threshold produced significantly different morphological parameters. This is most likely due to the heterogeneous and layered nature of bone as shown in Fig. 3. This significant change suggests that this small increase in threshold value crosses a significant point in the sample density, which is most likely related to a change in layer density.

140

Table 2. P-values for the difference between the three data sets of the measured morphometric parameters; t-test is for paired data sets using 2 tails.

	BV/TV	BS/TV	TbN	TbSp
Collagen vs Air	<0.001	<0.001	<0.001	<0.001
Collagen vs Water	<0.001	<0.001	<0.001	<0.001
Air vs Water	0.386	0.708	0.933	0.624

3.1 CT vs Archimedes

145 The two variables of main interest in bone research and clinical diagnosis is BV/TV and tissue density. Fig. 4 shows what the classical Archimedes method produces for this range of samples and what μ CT would produce in a non-invasive scan. The effect of the three thresholds is also shown and

agrees with the place where the bar is set in Fig. 1. If the density threshold is set at the organic tissue density level, there is marked deviation between μ CT and Archimedes results. Archimedes thresholds everything above the density of the suspending medium (1 in this instance for water) while μ CT sets the density at a level above 1 g/cm³ in all cases. Fig 4a (and also in figures 7 to 10 later on in this article) contains data and polynomial empirical model curves.

Figure 4

155

3.2 Microarchitectural parameters across BV/TV range

Fig 5 shows the behaviour of specific surface area BS/TV vs BV/TV for all 112 samples together with the data produced by Martin [5]. By overlaying the two sets of data we observe that the overall pattern is remarkably similar, with slight difference at the point where the apex is and the magnitude of values, which appear to be slightly higher overall for Martin's data compared to the current one. However, these are from two different techniques (histology vs. μ CT) and for two different tissues (human vs. elephant). The present data show a minimum specific surface area (~ 0.6 mm⁻¹) at BV/TV zero and 1 (the absolute minimum and maximum) and an apex (maximum) at BV/TV ~ 0.55 .

165

Figure 5

Fig. 6 shows the specific surface vs BV/TV relationship of the 31 samples imaged with demineralised bone tissue being present alongside normal bone tissue. The data show differences in the three conditions (air, water and collagen) considered here. When imaged in air and water, the data points largely overlap, suggesting that this difference in thresholding does not have a significant impact on the measurements of BV/TV and BS/TV. However, when collagen is taken as the background, the curves show distinct differences to the other two curves-- suggesting that towards the surface of the bone there is a lower density layer of epithelial tissue and osteoid. This lower density or less mineralised layer could be an important consideration in computational modelling studies of bone remodelling [1].

175

Figure 6

180 The direct outcome of the consequences of the bone dynamics regulated via the active surface can be seen in Fig. 7. The material density produced by μ CT and Archimedes is each plotted against BV/TV produced by these two methods. The result is a curve in the shape of a trough with lower densities for BV/TV ~ 0.6 . Archimedes thresholds precisely for a density = 1 g/cm^3 and above, and the other three for successively higher threshold densities. In accordance with the modelling by Berli et al. [1] and the bone kinetics it shows that bone at mid-range BV/TV has relatively higher remodelling rate, lower tissue age, resulting in higher organic content and lower tissue density.

Figure 7

190 Fig. 8-10 show the trends for the bone tissue densities (D_{mat}) and the microarchitectural parameters (BS/BV, TbTh, TbSp) across the broad BV/TV range. The BS/BV vs. BV/TV relationship declines rapidly to the value of zero as BV/TV approaches the value of 1 and at the other end of the range as BV/TV approaches zero the BS/BV approaches infinity. Fig. 8b shows again that the overall trend is the same for air and water and different for the collagen as background.

195 The relationship between the trabecular thickness and bone volume (Fig. 9) behaves inversely to the relationship between the trabecular spacing and bone volume (Fig. 10), both of which appear to follow a power law. The collagen threshold produces a noticeable shift from the air and water backgrounds for both the trabecular thickness (Fig. 9b) and the trabecular spacing (Fig. 10b) plots.

200 **Figure 8**

Figure 9

Figure 10

4. DISCUSSION

205 Micro-CT scanning is a powerful non-invasive and non-destructive structural analysis method which allows the inner architecture of bone to be examined in fine detail. However, its success is

contingent on calibration routines and appropriate protocols been used while deploying it. One such important methodological issues for micro-CT is setting the correct threshold level relevant to the tissue density so as to distinguish what is tissue and what is the surrounding medium, be it marrow, blood, water, or other organic material. The need to assess and set the right threshold has been commonly overlooked in the past.

In the present study we deal with two issues: (1) the question of having and setting an appropriate scanning thresholds level with 3 choices between air water and organic matter; and (2) the effect these three different backgrounds may have on a number of notable microarchitectural parameters used in bone mechanics and physiology; and we do so for samples across the broadest possible range of porosity values (for BV/TV in between 0 and 1). We have investigated the structural and microarchitectural relationships that exist within bone tissue across the whole spectrum of bone porosity, carried out using cone beam μ CT. Determination of these structural relationships is vital in understanding the mechanics of bone due to its cellular nature [7] and in understanding the remodelling rates at different sites within bone tissue [14]. Establishing typical ranges of normal trabecular architectural parameters can provide a useful tool in determining if a patient's bones are mechanically compromised, or at a greater risk of diseases such as osteoporosis. It has been shown that osteoporotic bone displays thinning or loss of trabeculae which contributes to a reduced fracture toughness [8,18].

The physical modality by which such bone level observations are made is inevitably CT scanning, which uses x-rays and thereby allows one to survey the structure in a non-invasive and non-destructive manner. The μ CT scanning we used here is based on the same principles like clinical scanning but of course in lab use it employs much more powerful x-ray radiation (which in clinical use would be harmful). The connection though between lab and clinical scanning is strong and the present data and results establish valuable trends for the behaviour of the various microarchitectural features across a wide range of porosity values (or BV/TV). By scanning samples and using three different backgrounds, we were able to establish that no significant differences in the produced histomorphometry parameters were seen between imaging in water or in air, suggesting that for biomechanical studies of small isolated specimens in the lab imaging in water is not a necessity for obtaining accurate micro-architectural data.

As limitations we can mention the use of elephant rather than human bone, which is also a mammal but with larger sized bones and consequently the absolute numbers given may not be representative of human tissue. It has however been demonstrated that there is a predictable offset in the

structural properties of bone tissue micro-architecture based on the relative sizes of the animals [19]
240 and from these facts possible adjustments can be made to predict what the present data values will
be for humans. The samples were also taken from just one animal, so they may lack the
interindividual variability that may have been evident otherwise. In an ideal scenario, this study
would be repeated using human bone samples taken from various sites around the body and using
multiple individuals representative of both sexes and a range of age groups. The clinical relevance
245 and translation of this work could be further improved in the future by producing and adding HU
units values [20]. The imaging resolution was insufficient to explore the vascular micro-architecture,
which has been suggested to be in length scale $<1 \mu\text{m}$ [17]. This is also part of the specific surface of
bone (sites for cellular activity for bone remodelling), the intracortical porosity of osteonal canals
and Volkmann canals within the cortical bone itself, which is in remodelling terms actively porous to
250 a significant extent. As shown by Fig. 5, we have produced BS/TV vs. BV/TV curves that are
remarkably similar and consistent with those previously reported by Martin [5]. Small differences at
the point where the apex of the curve is (peak) and the actual overall height are to be expected
considering possible differences between elephant and human bone and the two different
methodologies that have been used.

255 A comparison of the results throughout all parameters when the scan threshold is placed by using
the three backgrounds (air, water, collagen) showed that thresholding at the collagen level has the
greatest effect on the morphological results produced from the μCT . This suggests that bone density
varies with depth within the bone tissue and that lower density tissue exists nearest to the available
surface. It has also been shown that imaging in either water or air does not produce significantly
260 different results; this is an important discovery as it shows that, contrary to what is often
recommended, imaging dry or wet bone samples should not have a statistically significant impact on
the results. The differences seen between the collagen threshold versus the air and water may
suggest that the structure of bone varies with depth from the surface with low density material
being more superficial perhaps due to more recent remodelling activity, a fact which we have tried
265 to explore and exploit recently [1]. To a small extent this could also be an artefact from the partial
volume effect from μCT imaging; this occurs when the scan voxels at a boundary contain both the
sample and the background, which in turn reduces the density of the voxel. This however only
happens for just one layer of voxels, those at the edge which contain both bone and its surrounding
medium.

270

5. CONCLUSIONS

Setting the most appropriate scanning threshold is critical in producing accurate bone microarchitectural parameters by micro scanning, and we have shown here that values between the different sets of data differed by as much as 85% in some cases. Overall, the values produced for thresholds based on organic material deviated greatly from those based on air and water. We
275 believe that knowing this result is very useful for cases where bone is inspected with this non-destructive imaging method. The relationship between BS/TV vs. BV/TV in particular produced by μ CT scans can be used in the development of models that predict bone remodelling. Developing such models is vitally important in understanding how the skeleton behaves and could lead to
280 further understanding of the underlying mechanism that drives the remodelling process. It could also enable a more profound understanding of the underpinning processes which may help in diagnosis, an earlier identification of abnormal or diseased bone, or those that might be at greater fracture risk.

285 Acknowledgments

The tests were carried out in the Biomechanics laboratories of the Cranfield Forensic Institute of Cranfield University in Shrivenham, UK. The authors acknowledge the in-kind support of the Cranfield Forensic Institute and the Department of Comparative Biomedical Sciences (RVC) and ZSL Whipsnade Zoo for provision of the specimen.

290 Conflict of Interest

The authors declare that the research was conducted in the absence of any commercial or financial relationships that could be construed as a potential conflict of interest.

Author Contributions

Conceptualization: PZ, RC, GA, JH. Data curation: GA, PZ. Formal analysis: GA, PZ. Funding
295 acquisition: PZ, JH. Investigation: GA, PZ, RC, JH. Methodology: GA, PZ. Project administration: PZ. Resources: PZ, JH. Software: GA. Supervision: PZ, RC, JH. Validation: PZ, RC. Visualization: GA. Writing (original draft): GA, RC. Writing (review and editing): GA, PC, PZ, JH.

Funding

The authors acknowledge the support of the EPSRC (GR/N33225; GR/N33102; GR/ M59167) &
300 BBSRC (BB/C516844/1).

Data accessibility

Data for this manuscript when the article is in print will be available through the Cranfield University
CORD data depository and preservation system at <https://cranfield.figshare.com>

Ethical Approval

305 No HTA approval required

References

- 310 [1] M Berli, C Borau, O Decco, GJ Adams, RB Cook, JM Garcia Aznar, P Zioupos. Localized tissue mineralization regulated by bone remodelling: A computational approach. PLOS ONE 12(3) (2017) e0173228. doi.org/10.1371/journal.pone.0173228
- [2] GJ Adams, Quality factors at the material and structural level that affect the toughness of human cancellous bone. PhD dissertation, 2017, Cranfield University, UK.
<http://dspace.lib.cranfield.ac.uk/handle/1826/15952>
- 315 [3] P Zioupos, RB Cook, JR Hutchinson. Some basic relationships between density values in cancellous and cortical bone. Journal of Biomechanics, 41(9) (2008) 1961-8.
doi:10.1016/j.jbiomech.2008.03.025.
- [4] GJ Adams, RB Cook, JR Hutchinson, P Zioupos. Bone Apparent and Material Densities Examined by Cone Beam Computed Tomography and the Archimedes Technique: Comparison of the Two Methods and Their Results. Frontiers in Mechanical Engineering. 3 (2018)
320 doi.org/10.3389/fmech.2017.00023
- [5] RB Martin. Porosity and specific surface of bone. Critical reviews in biomedical engineering, 10(3) (1984) 179-222.
- [6] DP Fyhrie, NL Fazzalari, R Goulet, SA Goldstein. SA. Direct calculation of the surface-to-volume ratio for human cancellous bone. Journal of biomechanics. 26(8) (1993) 955-67.
325 doi.org/10.1016/0021-9290(93)90057-L.
- [7] L J Gibson. The mechanical behaviour of cancellous bone. Journal of Biomechanics, 18(5) (1985) 317-28. doi.org/10.1016/0021-9290(85)90287-8.
- [8] C Greenwood, J Clement, A Dicken, J Evans, I Lyburn, R Martin, K Rogers, N Stone, G Adams, P Zioupos. The micro-architecture of human cancellous bone from fracture neck of femur

- 330 patients in relation to the structural integrity and fracture toughness of the tissue, *Bone Reports*, 3 (2015) 67-75. doi: 10.1016/j.bonr.2015.10.001.
- [9] C Greenwood, J Clement, A Dicken, J Evans, I Lyburn, R Martin, K Rogers, N Stone, P Zioupos. Towards new material biomarkers for fracture risk, *Bone*, 93 (2016) 55-63. doi.org/10.1016/j.bone.2016.09.00. 6.
- 335 [10] C Greenwood, J Clement, A Dicken, J Evans, I Lyburn, R Martin, N Stone, P Zioupos, K Rogers. Age-related changes in femoral head trabecular microarchitecture, *Aging and Disease*, 9 (6) (2018) 976-87. doi: 10.14336/AD.2018.0124.
- [11] JD Currey, J.D. *Bones: Structure and Mechanics*, Princeton University Press, (2002) Princeton NJ.
- 340 [12] G Rouhi, W Herzog, L Sudaki, K Firoozbakhsh, M Epstein. Free Surface Density Instead of Volume Fraction in the Bone Remodeling Equation: Theoretical Considerations. *Forma*, 19 (2004) 165-82. doi:10.1016/j.ijengsci.2006.02.001.
- [13] WD Sharpe. Age changes in human bone: an overview. *Bulletin of the New York Academy of Medicine*, 55(8) (1979) 757-73. PMID: 385089; PMCID: PMC1807695.
- 345 [14] PR Buenzli, CD Thomas, JG Clement, P Pivonka. Endocortical bone loss in osteoporosis: the role of bone surface availability. *Int J Numer Method Biomed Eng*. 29(12) (2013) 1307-22. doi.org/10.1002/cnm.2567
- [15] LA Feldkamp, SA Goldstein, AM Parfitt, G Jasion, M Kleerekoper. The direct examination of three-dimensional bone architecture in vitro by computed tomography. *J Bone Miner Res*. 4(1) 350 (1989) 3-11. doi:10.1002/jbmr.5650040103.
- [16] P Zioupos, RB Cook, JR Hutchinson. More thoughts on the relationship between apparent and material densities in bone. *Journal of Biomechanics*. 42(6) (2009) 794-5. doi.org/10.1016/j.jbiomech.2009.01.014.
- [17] Y-B Yan, W Qi, J Wang, LF Liu, EC Teo, Q Tianxia, JJ Ba, W Lei. Relationship between 355 architectural parameters and sample volume of human cancellous bone in micro-CT scanning. *Medical engineering & physics*, 33(6) (2011) 764-9. doi:10.1016/j.medengphy.2011.01.014.
- [18] RB Cook, P Zioupos. The fracture toughness of cancellous bone. *J Biomech*. 42(13) (2009) 2054-60. doi: 10.1016/j.jbiomech.2009.06.001.
- [19] TM Ryan, CN Shaw. Trabecular bone microstructure scales allometrically in the primate

360 humerus and femur. *Proceedings of the Royal Society B: Biological Sciences*, 280(1758) (2013) 20130172. doi:10.1098/rspb.2013.0172

[20] P Mah, TE Reeves, D McDavid. Deriving Hounsfield Units using grey levels in cone beam computed tomography. *Dentomaxillofacial Radiology* 39(6) (2010) 323-35. doi:10.1259/dmfr/19603304.

365 [21] D Ruffoni, P Fratzl, P Roschger, K Klaushofer, R Weinkamer. The bone mineralization density distribution as a fingerprint of the mineralization process. *Bone* 40, (2007) 1308–1319. doi:10.1016/j.bone.2007.01.012

370 **FIGURE CAPTIONS**

Figure 1. Grey level histogram showing: (a) the peaks labelled for air, water, demineralised sample and native sample. The RED line half way between the BLUE ones (peaks) is where the threshold is placed: (b) when air is taken as the background; (c) when water is taken as the background; and (d) when the demineralised sample (organic matter) is taken as the background. It is clear in this illustration that for whole native bone tissue the border line (BL- arrow) for real bone is between the two peaks for water and collagen, that is where water ‘ends’ and bone tissue (including small amounts of osteoid and epithelial tissue) ‘begins’. Unfortunately, in practice and in all cases this trough between water and collagen is never apparent or easy to define, it is buried in the tail end of the water peak. It has only become clear here because we used this technique of demineralising some of the same bone tissue to create a peak for truly native demineralised bone tissue. Notably, to create a noticeable peak a substantial mass of demineralised bone is needed because collagen is much lighter than mineral and less able to absorb x-rays. Importantly, when using the Archimedes technique (immersion and suspension in a medium [2-4]) the actual threshold (red bar) is on the water peak itself (Arch -arrow) where the blue bar is on the water peak in (c).

385 Figure 2. (a) QRM Calibration phantom images and histogram (data in Table 1); (b) the resultant calibration curve (using the calibration certificate nominal values) which produces density values from CT grey level (the error bars shown are \pm SD).

Figure 3. Microscope images (backscattered SEM) showing the mosaic of micro-compartments of bone tissue in: (a) cortical bone (cross section of femur, 60 yr old male) and (b) in cancellous bone (modified from Adams et al. [4] and original from Ruffoni et al. [21]). The various

390

tissue compartments are labelled as '1' being the more recent, towards '5' being the older one using the grey level scale whereby the lighter the area the denser it is and the older the tissue age. If the threshold is raised to exclude bone pockets such as '1' the microarchitectural analysis would then apply to the part of bone within the red-dotted area, which becomes then the 'new' bone surface.

395 Figure 4. BV/TV and D_{mat} bone material density (g/cm^3) from Archimedes immersion method and from μ CT with 3 different thresholds. (a) BV/TV, water (open red diamonds) and air (blue solid circles) produce similar results, the collagen background (solid green squares) shifts the data significantly downwards, BV TV from CT is severely eroded when collagen is the threshold and has values between 30-50% smaller than BV/TV by Archimedes especially for intermediate BV/TV values
400 (Black dashed line is line of equality; air: $y = 0.697x + 0.299x^9$, $R^2 = 0.971$; water: $y = 0.687x + 0.314x^9$, $R^2 = 0.971$; collagen: $y = 0.418x + 0.527x^9$, $R^2 = 0.964$); (b) D_{mat} the water threshold produces results with greater scatter (probably through affecting absorption of the x-rays), the curves for air and collagen are practically identical. For high D_{mat} values (BV/TV near 0 or 1) the CT and Archimedes techniques produce equal values (on average) but for lower density bone samples (intermediate
405 BV/TV) the CT overestimates D_{mat} compared to Archimedes. (Black dashed line is line of equality; air: $y = 0.924 + 0.524x$, $R^2 = 0.686$; water: $y = 0.453 + 0.756x$, $R^2 = 0.428$; collagen: $y = 0.951 + 0.510x$, $R^2 = 0.726$).

Figure 5. Specific surface BS/TV vs. bone volume BV/TV measured using μ CT for all 112 samples from an elephant femur. The samples having $D_{app} > 1.3$ are encircled as this is the BV/TV level
410 beyond which histology would have conventionally defined it as being cortical bone. Black solid parabola is the behaviour of data produced by Martin [5] added here for comparison (similar to Berli et al. [1]).

Figure 6. Specific surface (BS/TV) vs. bone volume (BV/TV) measured using μ CT on 31 samples, those where both mineralised and demineralised bone was present in the scan and in three
415 different background thresholds. Red open diamonds = imaged in water, blue solid circles = imaged in air and green solid squares = with a collagen background. For the remodelling process working through an active surface, relatively more bone tissue volume can be accessed at the intermediate range of BV/TV values, not at the two extremes (cancellous and cortical). The values for BS/TV at its peak derived from the collagen background are 30% less than those derived with respect to water and air backgrounds.
420

Figure 7. Material density (D_{mat}) vs. BV/TV, by μ CT, for air (blue), water (red) and collagen (green) backgrounds and by using Archimedes immersion method (black). Remodelling working

through the available specific surface, according to the model by Berli et al. [1], modulates the mineral content (tissue density) accordingly. All four methods indicate that in mid-range BV/TV the organic content is relatively higher and the tissue density lower as a result. The values of D_{mat} at the trough are higher by 32% for water, 68% for air and 84% for collagen as backgrounds with respect to the $D_{mat} / (BV/TV)$ behaviour derived by the Archimedes method. (Archimedes: $D = 2.02 - 0.977 (BV/TV) + 0.749 (BV/TV)^3 + 0.303 (BV/TV)^9$, $R^2 = 0.767$; air: $D = 1.93 - 0.450 (BV/TV) + 0.675 (BV/TV)^2 - 0.151 (BV/TV)^9$, $R^2 = 0.734$; water: $D = 1.88 - 0.332 (BV/TV) + 0.519 (BV/TV)^3$, $R^2 = 0.446$; collagen: $D = 1.83 + 0.196 (BV/TV) + 0.054 c(BV/TV)^3$, $R^2 = 0.496$).

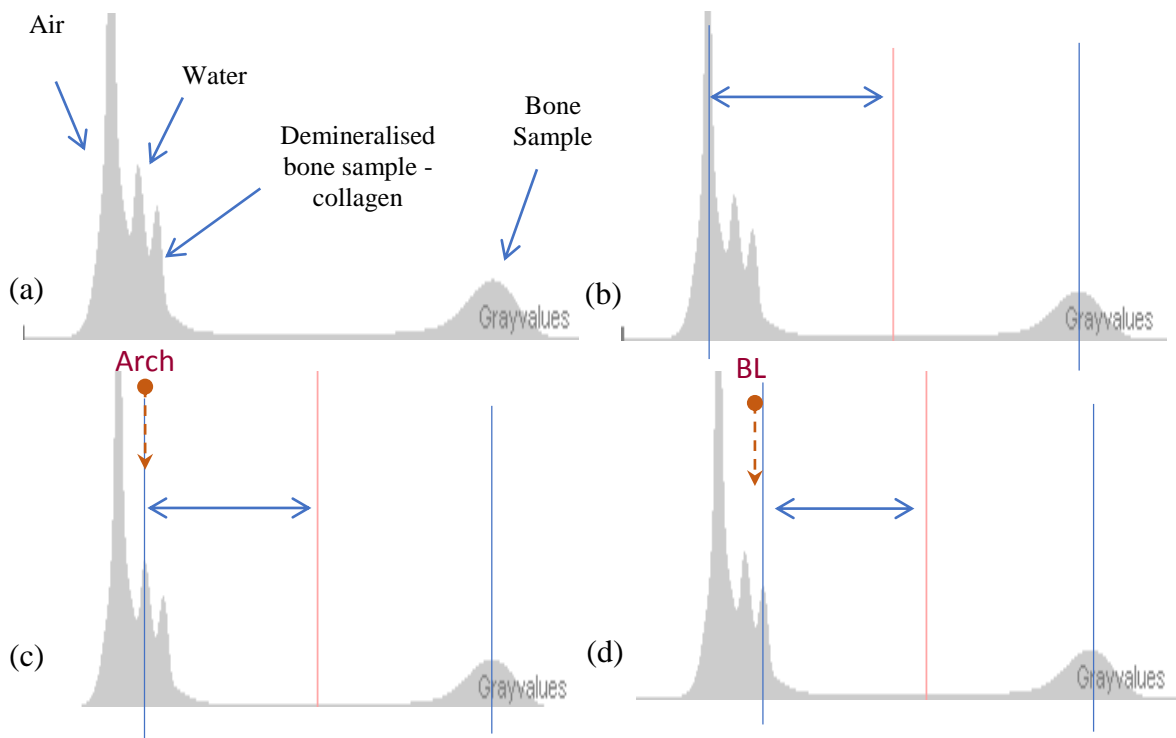
Figure 8. (a) BS/BV vs. BV/TV for the full range of 112 samples and (b) for the sub-group of 31 samples measured with different backgrounds: Red open diamonds = in water, blue solid circles = in air and green solid squares = with a collagen background. The values for BS/TV from collagen backgrounds across the BV/TV range are lower by 25% to 30% with respect to the values produced with air and water backgrounds. Naturally in the absence of any pores and voids the absolute limit for BS/BV is zero as BV/TV tends to 1. It is a simple corollary of geometry and morphometrics that the specific surface area (area over the enclosed volume) of a particle tends towards very high values for any geometrical scheme regardless if it is bone or anything else (the finer the power the highest specific surface area; $Area/Volume = f(R^2)/f(R^3) \sim 1/R$ with R approaching zero the value approaches infinity).

Figure 9. (a) Trabecular thickness (TbTh) vs. BV/TV for the full range of 112 samples and (b) for the sub-group of 31 samples measured with different backgrounds: Red open diamonds = in water, blue solid circles = in air and green solid squares = with a collagen background. The values for TbTh produced from collagen background are between 40% and 85% higher than the ones produced on air and water backgrounds.

Figure 10. (a) Trabecular spacing (TbSp) vs. BV/TV for the full range of 112 samples and (b) for the sub-group of 31 samples measured with different backgrounds: Red open diamonds = in water, blue solid circles = in air and green solid squares = with a collagen background. The values for TbSp are lower at the higher end of BV/TV values for collagen background by up to 85% comparing to air and water backgrounds.

FIGURES

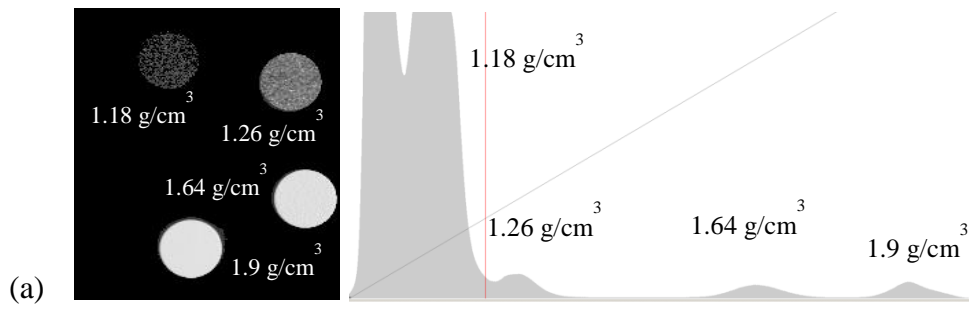
455



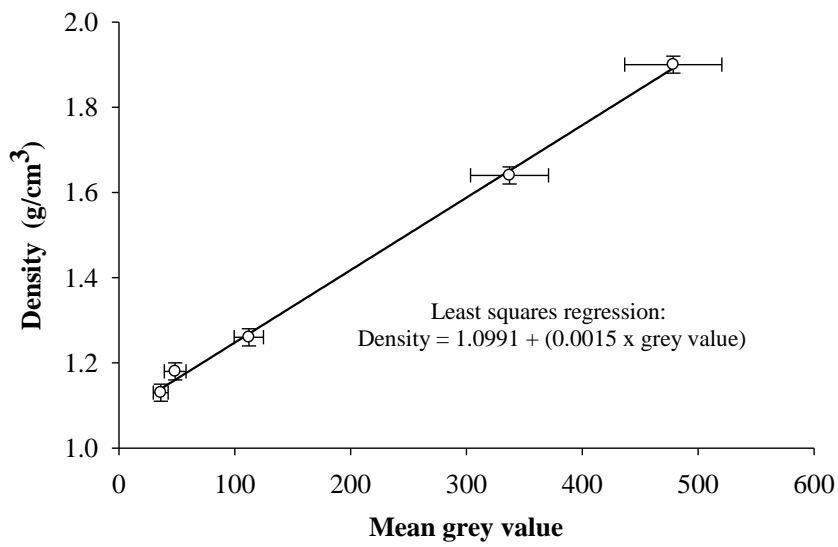
460

FIGURE 1

465



470

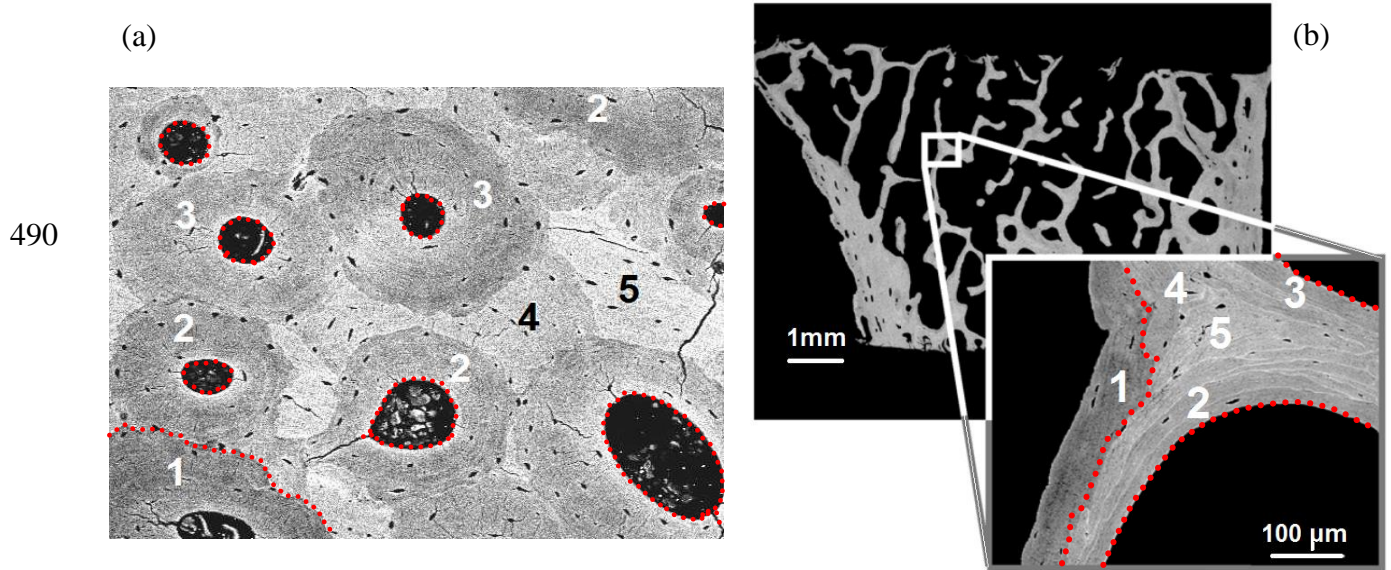


475

480

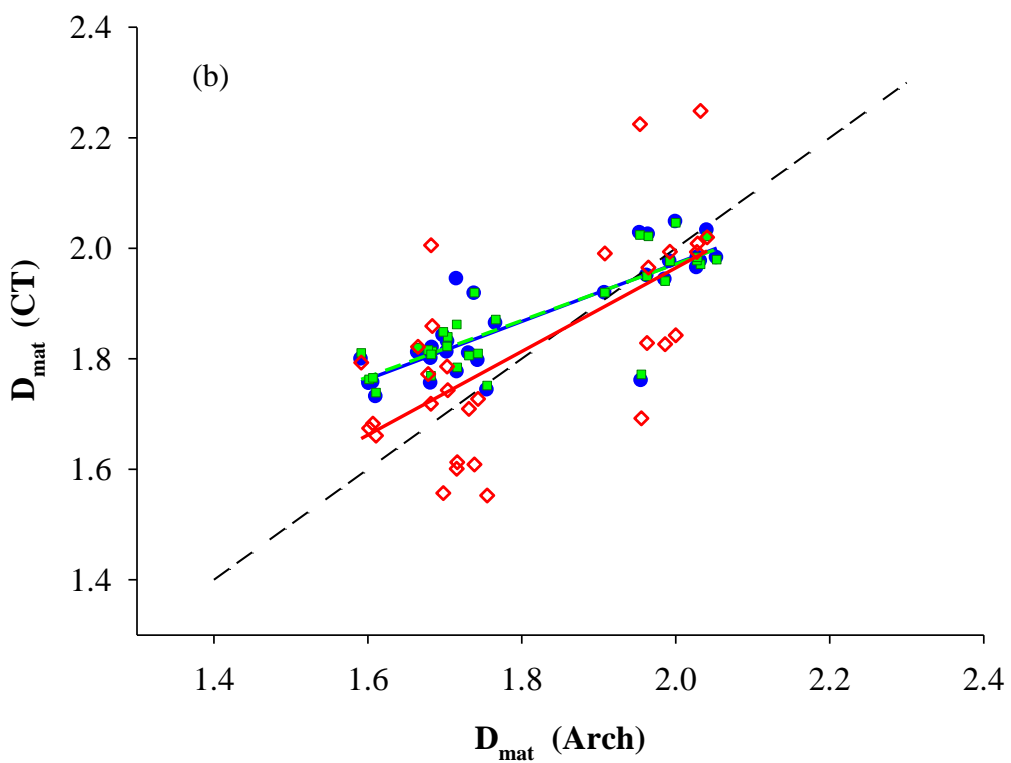
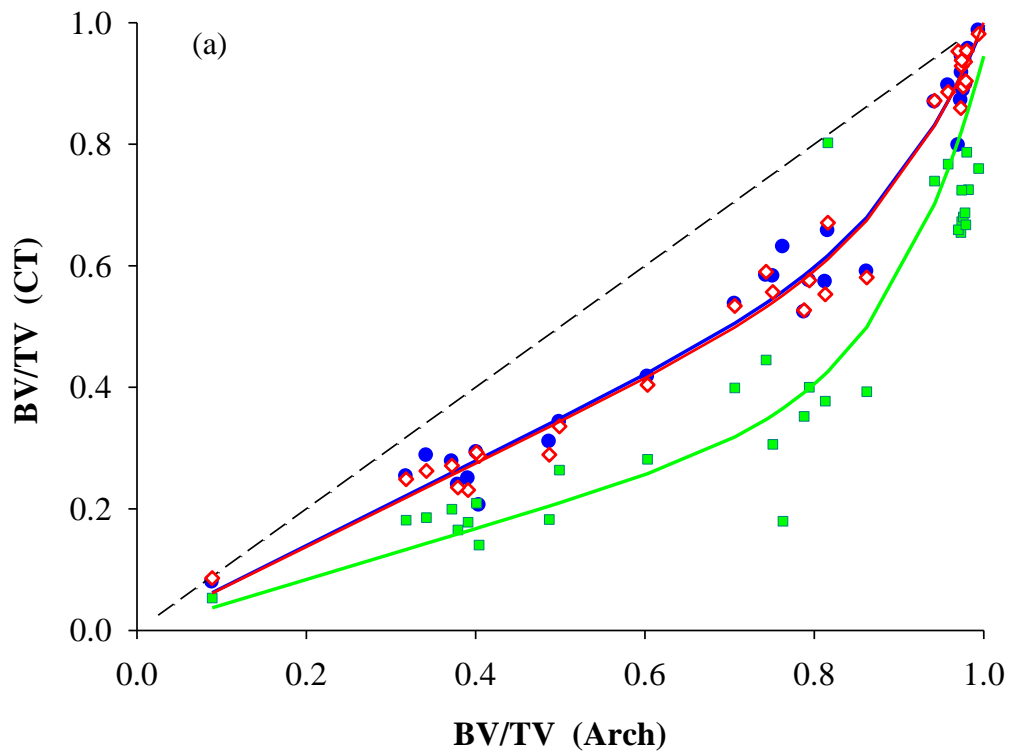
FIGURE 2

485



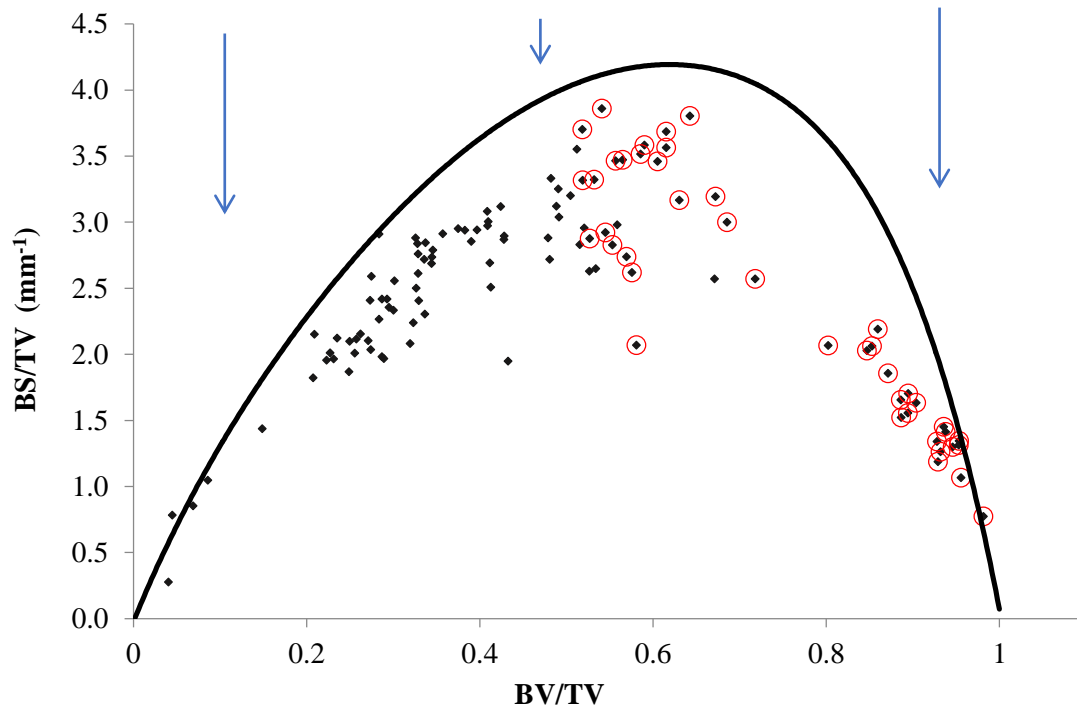
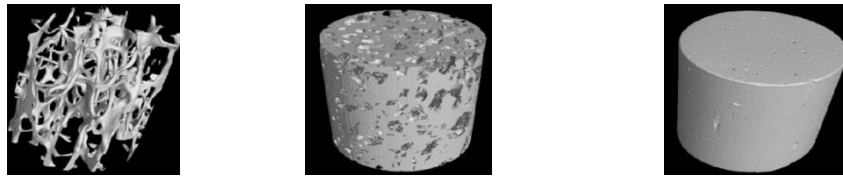
495

500 FIGURE 3



505 FIGURE 4

510



515

FIGURE 5

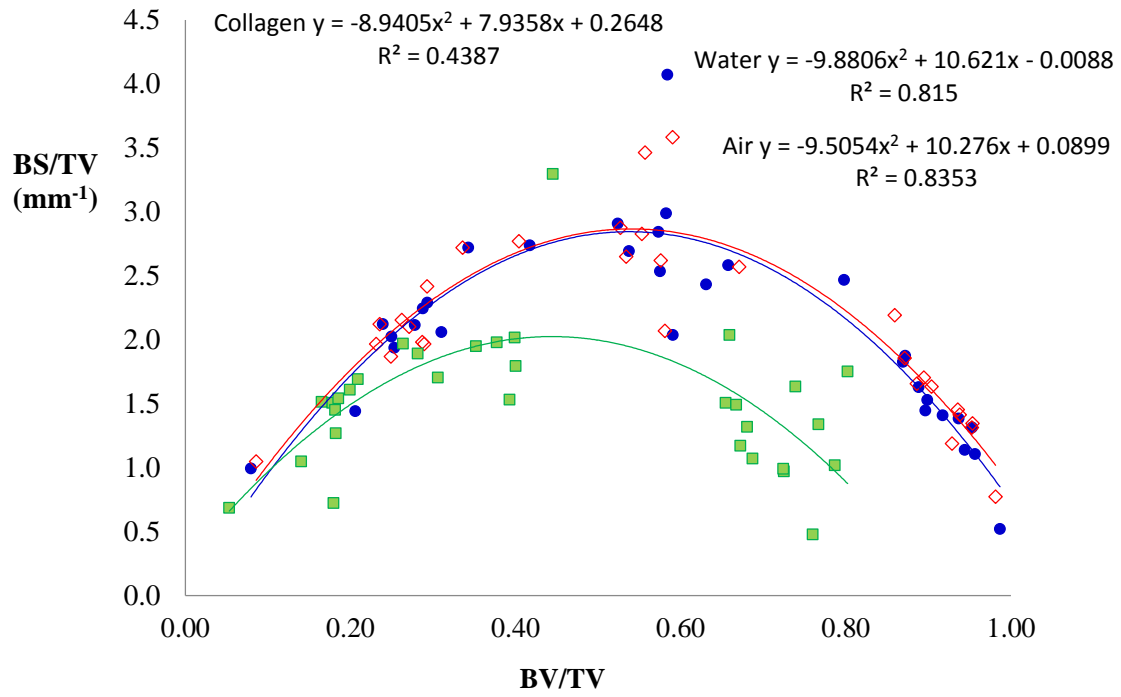
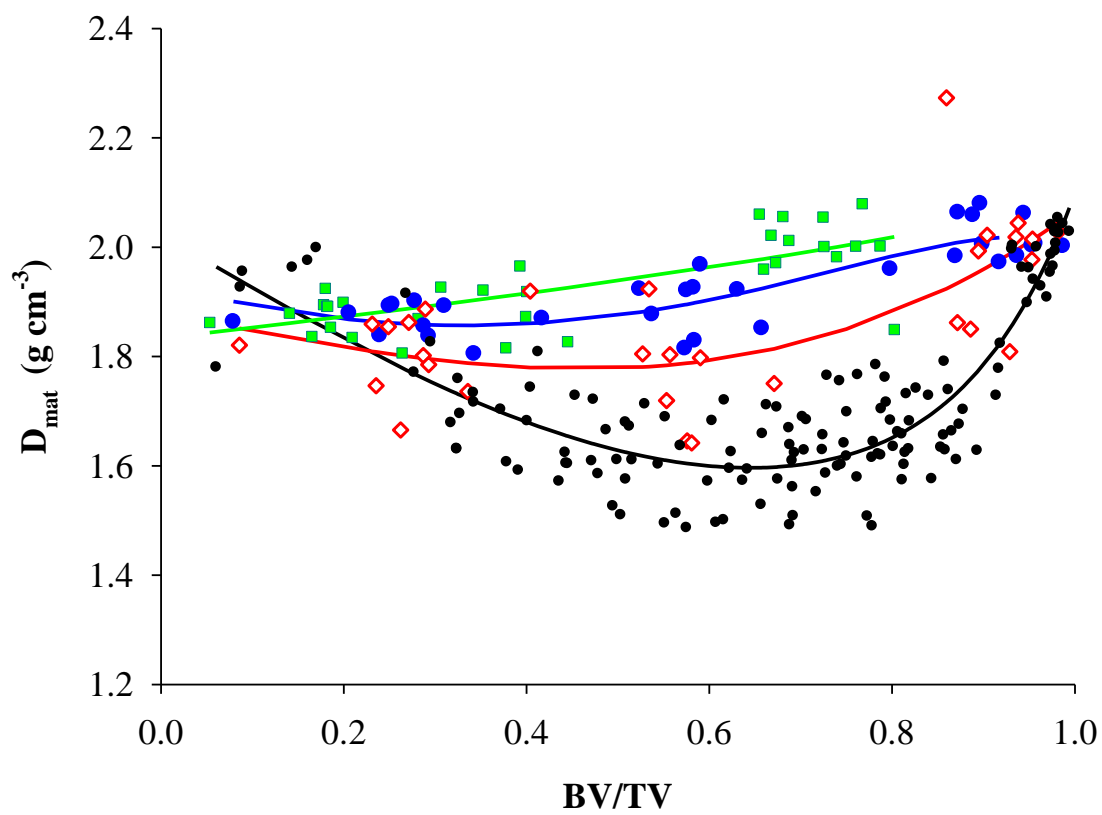


FIGURE 6



530

FIGURE 7

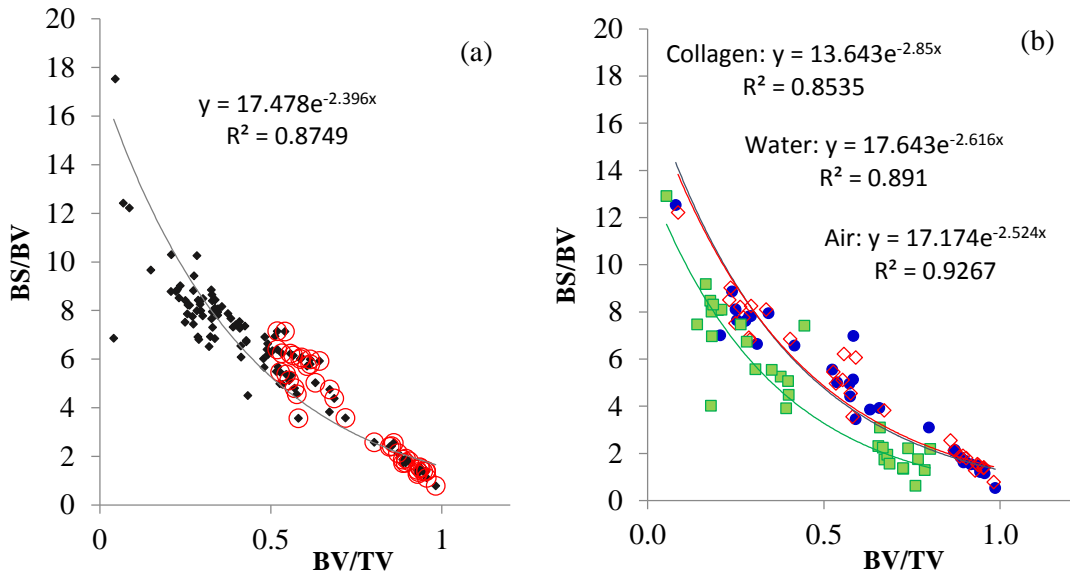


FIGURE 8

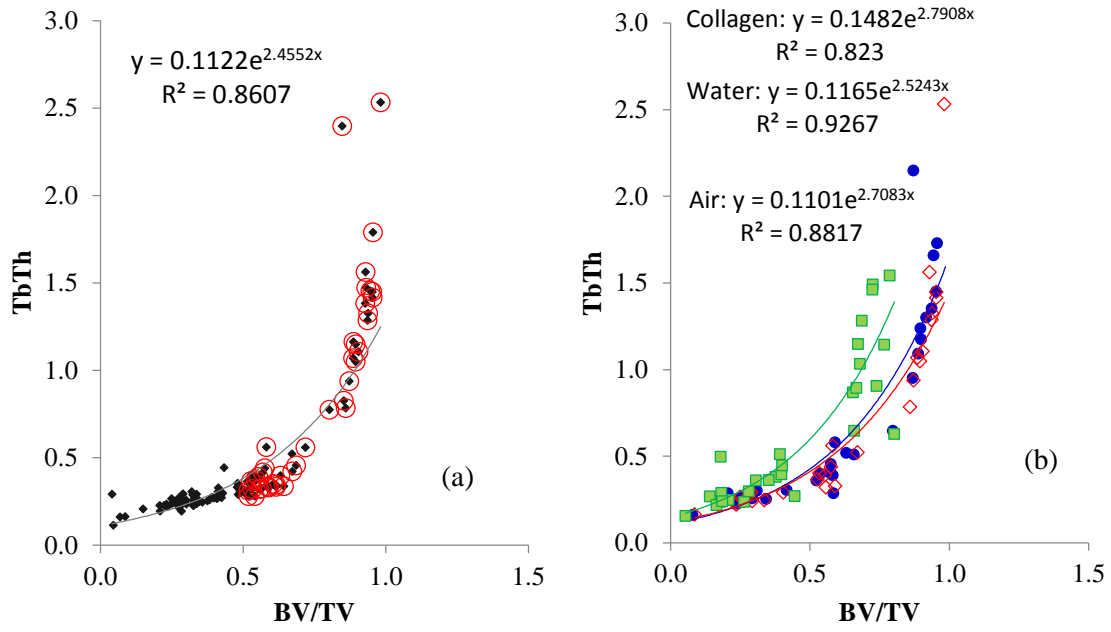


FIGURE 9

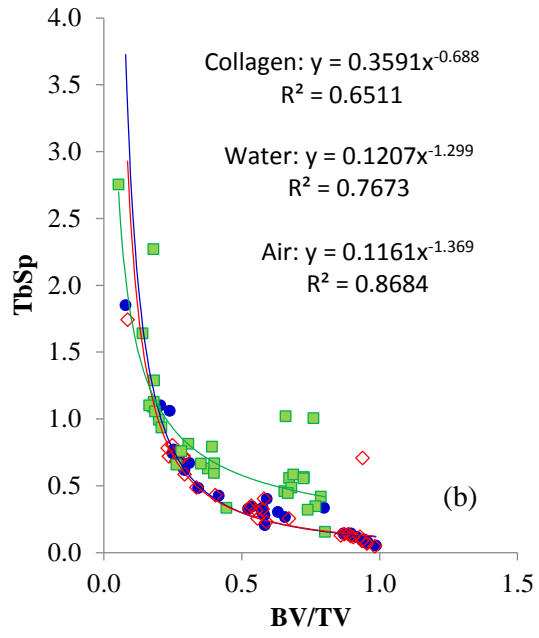
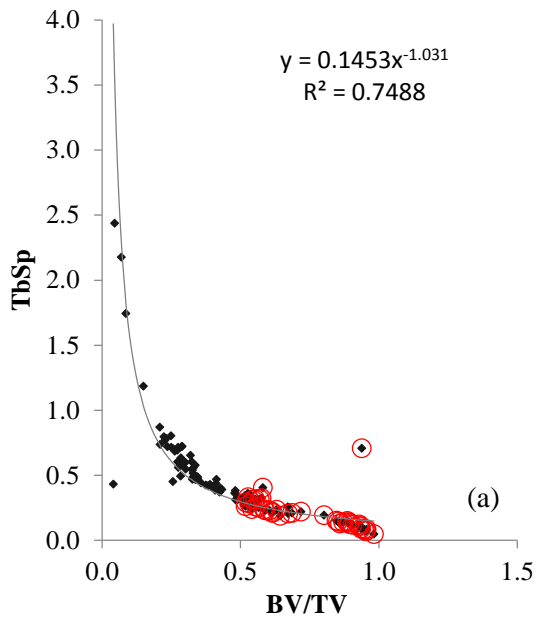


FIGURE 10

Microarchitecture and morphology of bone tissue over a wide range of BV/TV assessed by micro-computed tomography and three different threshold backgrounds

Adams GJ^a, Cook RB^b, Hutchinson JR^c, Zioupos P^a *

a Cranfield Forensic Institute, Cranfield University, Defence Academy of the UK, Shrivenham, UK

b nCATS, School of Engineering Science, University of Southampton, Southampton, UK

c Structure and Motion Laboratory, Department of Comparative Biomedical Sciences, The Royal Veterinary College, Hatfield, UK

Abstract

The microarchitecture of bone both results from and in turn affects the remodelling process. Bone-specific surface, for instance, is one of these important microarchitectural parameters because remodelling is also considered to be a surface-mediated phenomenon (Berli et al. 2017). An understanding of these structural parameters across the widest possible range of porosity is essential to illuminating how bone reacts to disease, in different skeletal sites and in either its cancellous or cortical forms. 112 samples from an elephant femur were examined by micro-computed tomography (μ CT), 31 of which contained both mineralised and demineralised tissue. A critical factor in all scans is setting the correct threshold (with background the surrounding medium) and hence 3 different backgrounds were used: air, water and collagen. The effect of the 3 background thresholds on the physical characteristics of bone (BS/TV, BS/BV, TbSp, TbTh, D_{mat} , vs BV/TV) was then determined. The results showed that using a threshold set by the collagen background had a profound effect on the histomorphometry bone parameters when assessed by μ CT. However, the differences between air and water were not significant, suggesting that comparable data can be produced in a laboratory environment when scanning porous bone samples under either wet or dry conditions-- counter to common belief. Determining which is more suitable, air or water, in laboratory and in clinical μ CT imaging is important to improve the quality and relevance of biomechanics research. The data with collagen as the threshold were illuminating as they showed that remodelling rates and the relative organic to mineral presence varied with BV/TV, concurring with some other recent studies [2,3,4].

Keywords: Bone; cancellous; Cortical; density; Porosity; BV/TV; Specific surface; μ CT

* Corresponding author: p.zioupos@cranfield.ac.uk

1. INTRODUCTION

Determination of the structural characteristics of bone is essential in understanding bone's mechanical properties, rates of remodelling, or adaptation, and its susceptibility to disease. We have recently published [1] a new computational paradigm to illustrate that the local mineralisation patterns in bone follow certain rules, whereby the mineral content (through a diffusion via the bone active surface area) depends on the depth from the surface and the amount of active surface that is available. This model explained in detail some fundamental observations [3] we published in 2008 in which bone material density varies with BV/TV (bone volume/total volume of bone). The plot of bone material density vs. apparent density showed a bifurcating curve shaped like a 'boomerang' [3] showing that bone has the highest material density values for the lowest (cancellous) and highest (cortical) BV/TV values. This behaviour which was produced with the Archimedes principle technique (submersion in fluid to produce material density values) was later on corroborated with another independent technique which was both non-invasive and non-destructive, namely the use of microCT scanning [4]. Micro-CT scanning is a powerful method which can both confirm the densities bifurcating curve and also produce microarchitectural parameters across the full range of porosities. Three of the most important features of bone structure are the porosity, specific surface, and density [3,5,6]. Porosity is the void volume per unit volume of bone, which is often expressed as its inverse BV/TV (bone volume/total volume). Specific surface (BS/TV) is the total internal surface area per unit volume of bone tissue [5]. Density can be considered in two ways. Firstly, as apparent density (D_{app}), this can be defined as the mass over the whole volume of the sample, and its nearest equivalent in scanning is the bone volume mineral density (BMD). Secondly, as material density (D_{mat}), which can be defined as the mass of the bone over the volume occupied by the material itself, with its nearest equivalent in scanning being the tissue mineral density (TMD). BV/TV is a dimensionless ratio, BS/TV has the units cm^{-1} , and both densities have the same units g/cm^3 . BV/TV and D_{mat} are important because bone's primary role within the body is as a structural material in both its cortical or cancellous (cellular) forms [7]. We have recently argued that an understanding of how D_{mat} varies with BV/TV is important in bone disease specifically when trying to understand the impact of osteoporosis [1-4]; and also important to understand the relationship between the other histomorphometry variables well and within 'normal' bone, so that irregularities in diseased bone can be identified [8-10].

One of the important histomorphometric parameters is active surface area because it is widely accepted that during the remodelling process, osteoclasts and osteoblasts act primarily through the openly accessible active surface available within bone tissue [11]. This remodelling effect is surface-

mediated either because the process is one where the cells have to be physically present and reach
35 a certain area, or where the metabolites need to diffuse across a boundary in and out of the bone
tissue into the medium. The level of activity of the cells is hormonally and metabolically driven and is
related to the total area over which the cells can act. As such the total BS/TV will impact on the
resultant rate of bone remodelling at specific sites [12,13]. BS/TV is determined by the micro-
40 architecture of bone including all places where there is a void, such as osteocyte lacunae, osteonal
canals and trabecular structure. Models of bone remodelling in the cortical regions of bone with
variations in the specific surface have shown that with a higher specific surface the rate of
remodelling is increased [14]. Better knowledge of the variations in specific surface for both cortical
and cancellous regions can help in improving the quality and accuracy of computational modelling of
bone remodelling which in turn can help with the understanding of bone condition in health or
45 disease. This was recently demonstrated using a computational approach to simulate the
remodelling process of bone with a dependence on the surface area [1]. The relationship between
the porosity and specific surface of bone has been previously investigated by Martin [5] in an
invasive way by using a series of histological slices. However, this method is time-consuming and
destructive so is not ideal in research and clearly impossible in clinical settings. The method also
50 carries limitations in resolution and inherent error as it is limited by slice thickness. By using μ CT this
relationship can be examined more easily with a potentially higher accuracy [15]. μ CT can also
access all internal structure by being 'optically' invasive throughout and that includes both open and
closed cells. However, μ CT is not without its own limitations in the sense that the reproducibility of
the results is critically dependent on the set-up parameters. One of these parameters is the
55 threshold background level, which can be the surrounding medium (air, water, fat) or even a certain
degree of mineralisation starting from organic matrix with no mineral at all, the osteoid (collagen).
Here we investigate bone microarchitectural parameters produced by μ CT across a very wide range
of porosities and as a function of this porosity level. We postulate that a more fundamental
knowledge of the inner workings of bone at the microarchitecture may result by understanding the
60 interplay between porosity and the other basic microarchitectural parameters and that can come by
controlling more precisely the different scanning threshold level backgrounds which define where
bone starts and where bone ends.

2. MATERIALS & METHODS

65 2.1 Specimens

In this study, samples were taken from the right femur of an adult Asian elephant (3432 kg, 24 years old). The advantage of using the femur of such a large mammal is that a large number of samples (n=112) over a wide range of BV/TVs (0.04-0.98) can be taken. The suitability of this tissue was confirmed in previous studies [3,16]. The specimen was collected shortly after the animal's
70 euthanasia (for reasons unrelated to this study) at ZSL Whipsnade Zoo (Bedfordshire, UK) and frozen (-20°C) until testing. The samples were cut in either cylindrical cores or cubes approximately 10mm³, larger than the minimum size recommended by [18]. Full preparation details can be found in our previous work [2,3,15]. In a subsection of samples (n=31) a 2mm thick slice was taken from the bottom of each sample and submerged in EDTA for 168hrs (7 days) with daily changes to fully
75 demineralise the slice. This demineralisation process left behind undamaged organic matrix (which is mostly collagen), which could then be used to provide a threshold for the organic bone material during μ CT scanning. The known density of this matrix was approximately 1.1 g/cm³ and this was confirmed with the Archimedes method similar to previous application [3]. All samples were stored frozen (-20°C) until testing and were allowed to defrost for 2hrs prior to imaging.

80 2.2 Imaging- μ CT

All samples were imaged using a cone beam μ CT scanner, Nikon XTEK XT H 225 (Nikon Metrology, Herts HP23 4JX, UK). The samples were imaged in ABS plastic sample holders at 50 kV, 65 μ A. The resultant voxel size was \sim 16 μ m, making them suitable to determine the samples' morphology with adequate resolution [17]. All 112 samples were imaged whilst fully submerged in deionised water.
85 The 31 samples were additionally imaged in air with both their mineralised volumes and the demineralised slices being present in the vials. All scans were manually reconstructed using CT Pro 3D. During reconstruction, conditions were optimised to reduce beam hardening.

Figure 1

90

The effect from using the three different backgrounds to produce grey level thresholds is shown in fig. 1. By using a different threshold, there is a virtual shift at the point where the perceived surface of the bone is. As the density of the background increases so does the threshold grey value which is placed halfway between the chosen peaks. As can be seen in the histograms of Fig. 1, there is

95 potentially a noticeable shift in the position of the 'bone' threshold for the three backgrounds consisting of air, water and organic matrix (collagen).

2.3 Image Analysis

Image analysis was carried out using VGSTUDIO MAX 2.2. Regions of interest (ROI) were taken from the centre of each sample $\sim 9 \text{ mm}^3$ to exclude any external surfaces from the scan. These surfaces, which have been introduced during the sample preparation process, were excluded as the software would consider them in the BS/TV calculations and therefore give erroneous results. A surface determination was performed using the grey level of an internal void as the background and the largest void-less section of bone, as per the manufacturers' recommendations. This thresholding process introduces a surface threshold at an intermediate point between the average grey values of these two sections. For the samples imaged with a collagen slice, the collagen was used as the background. After the surface determination an automatic morphometric report was exported. This contained: bone volume (BV/TV), specific surface (BS/TV), mean trabecular thickness (TbTh), mean trabecular number (TbN), and mean trabecular spacing (TbS).

From the histogram the mean, mode, minimum and maximum grey level were recorded to be used in calculation of the material density. A QRM-MicroCT-HA (QRM GmbH Dorfstrasse 4, 91096, Moehrendorf, Germany) calibration phantom was imaged and reconstructed under the same conditions in order to determine D_{mat} . Determination of material density is more favourable than deriving Hounsfield (HU) units, which are typically used in medical CT imaging, as HU is an x-ray specific expression of a materials linear attenuation coefficient and does not have any consistent conversion to physical density measurements. Therefore, using material density enables for comparison with physical density measurements that HU otherwise does not.

2.4 Density Calibration

Fig. 2 shows the histogram of the QRM HA calibration phantom alongside the 3D image of the scan, both obtained using VGSTUDIO. Within VGSTUDIO, each density was isolated and the average grey scale was determined and plotted against the density provided by the supplier. This provided a calibration curve from which the density of the bone samples could be determined. The average grey value of each sample was measured and using the calibration curve D_{mat} was determined (Fig.2b).

125 **Table 1. Properties of QRM calibration phantom.**

Sample	Mean grey	Density (g/cm^3)	Mineral %
Standard 1	36.10	1.13	0

Standard 2	48.60	1.18	0.42
Standard 3	112.20	1.26	15.89
Standard 4	337.20	1.64	48.29
Standard 5	478.45	1.90	63.17

Figure 2

Figure 3

130 **3. RESULTS**

A statistical comparison of the three different thresholds is shown in Table 2. The results of the comparison showed that the air and water thresholds were not statistically different when comparing the two datasets. This suggests that imaging bone in air and in water using μ CT produced no significant difference across the full range of bone porosities. A comparison of the three
 135 thresholds showed that increasing the value to the collagen threshold produced significantly different morphological parameters. This is most likely due to the heterogeneous and layered nature of bone as shown in Fig. 3. This significant change suggests that this small increase in threshold value crosses a significant point in the sample density, which is most likely related to a change in layer density.

140

Table 2. P-values for the difference between the three data sets of the measured morphometric parameters; t-test is for paired data sets using 2 tails.

	BV/TV	BS/TV	TbN	TbSp
Collagen vs Air	<0.001	<0.001	<0.001	<0.001
Collagen vs Water	<0.001	<0.001	<0.001	<0.001
Air vs Water	0.386	0.708	0.933	0.624

3.1 CT vs Archimedes

145 The two variables of main interest in bone research and clinical diagnosis is BV/TV and tissue density. Fig. 4 shows what the classical Archimedes method produces for this range of samples and what μ CT would produce in a non-invasive scan. The effect of the three thresholds is also shown and agrees with the place where the bar is set in Fig. 1. If the density threshold is set at the organic tissue density level, there is marked deviation between μ CT and Archimedes results. Archimedes

150 thresholds everything above the density of the suspending medium (1 in this instance for water)
while μ CT sets the density at a level above 1 g/cm³ in all cases. Fig 4a (and also in figures 7 to 10 later
on in this article) contains data and [polynomial empirical](#) model curves.

Figure 4

155

3.2 Microarchitectural parameters across BV/TV range

Fig 5 shows the behaviour of specific surface area BS/TV vs BV/TV for all 112 samples together with
the data produced by Martin [5]. By overlaying the two sets of data we observe that the overall
pattern is remarkably similar, with slight difference at the point where the apex is and the
160 magnitude of values, which appear to be slightly higher overall for Martin's data compared to the
current one. However, these are from two different techniques (histology vs. μ CT) and for two
different tissues (human vs. elephant). The present data show a minimum specific surface area (~ 0.6
mm⁻¹) at BV/TV zero and 1 (the absolute minimum and maximum) and an apex (maximum) at BV/TV
 ~ 0.55 .

165

Figure 5

Fig. 6 shows the specific surface vs BV/TV relationship of the 31 samples imaged with demineralised
bone tissue being present alongside normal bone tissue. The data show differences in the three
170 conditions (air, water and collagen) considered here. When imaged in air and water, the data points
largely overlap, suggesting that this difference in thresholding does not have a significant impact on
the measurements of BV/TV and BS/TV. However, when collagen is taken as the background, the
curves show distinct differences to the other two curves-- suggesting that towards the surface of the
bone there is a lower density layer of epithelial tissue and osteoid. This lower density or less
175 mineralised layer could be an important consideration in computational modelling studies of bone
remodelling [1].

Figure 6

180 The direct outcome of the consequences of the bone dynamics regulated via the active surface can
be seen in Fig. 7. The material density produced by μ CT and Archimedes is each plotted against
BV/TV produced by these two methods. The result is a curve in the shape of a trough with lower
densities for BV/TV ~ 0.6 . Archimedes thresholds precisely for a density = 1 g/cm^3 and above, and the
other three for successively higher threshold densities. In accordance with the modelling by Berli et
185 al. [1] and the bone kinetics it shows that bone at mid-range BV/TV has relatively higher remodelling
rate, lower tissue age, resulting in higher organic content and lower tissue density.

Figure 7

190 Fig. 8-10 show the trends for the bone tissue densities (D_{mat}) and the microarchitectural parameters
(BS/BV, TbTh, TbSp) across the broad BV/TV range. The BS/BV vs. BV/TV relationship declines rapidly
to the value of zero as BV/TV approaches the value of 1 and at the other end of the range as BV/TV
approaches zero the BS/BV approaches infinity. Fig. 8b shows again that the overall trend is the
same for air and water and different for the collagen as background.

195 The relationship between the trabecular thickness and bone volume (Fig. 9) behaves inversely to the
relationship between the trabecular spacing and bone volume (Fig. 10), both of which appear to
follow a power law. The collagen threshold produces a noticeable shift from the air and water
backgrounds for both the trabecular thickness (Fig. 9b) and the trabecular spacing (Fig. 10b) plots.

200 **Figure 8**

Figure 9

Figure 10

4. DISCUSSION

205 Micro-CT scanning is a powerful non-invasive and non-destructive structural analysis method which
allows the inner architecture of bone to be examined in fine detail. However, its success is
contingent on calibration routines and appropriate protocols been used while deploying it. One such
important methodological issues for micro-CT is setting the correct threshold level relevant to the
tissue density so as to distinguish what is tissue and what is the surrounding medium, be it marrow,

210 blood, water, or other organic material. The need to assess and set the right threshold has been commonly overlooked in the past.

In the present study we deal with two issues: (1) the question of having and setting an appropriate scanning thresholds level with 3 choices between air water and organic matter; and (2) the effect these three different backgrounds may have on a number of notable microarchitectural parameters used in bone mechanics and physiology; and we do so for samples across the broadest possible range of porosity values (for BV/TV in between 0 and 1). We have investigated the structural and microarchitectural relationships that exist within bone tissue across the whole spectrum of bone porosity, carried out using cone beam μ CT. Determination of these structural relationships is vital in understanding the mechanics of bone due to its cellular nature [7] and in understanding the remodelling rates at different sites within bone tissue [14]. Establishing typical ranges of normal trabecular architectural parameters can provide a useful tool in determining if a patient's bones are mechanically compromised, or at a greater risk of diseases such as osteoporosis. It has been shown that osteoporotic bone displays thinning or loss of trabeculae which contributes to a reduced fracture toughness [8,18].

225 The physical modality by which such bone level observations are made is inevitably CT scanning, which uses x-rays and thereby allows one to survey the structure in a non-invasive and non-destructive manner. The μ CT scanning we used here is based on the same principles like clinical scanning but of course in lab use it employs much more powerful x-ray radiation (which in clinical use would be harmful). The connection though between lab and clinical scanning is strong and the present data and results establish valuable trends for the behaviour of the various microarchitectural features across a wide range of porosity values (or BV/TV). By scanning samples and using three different backgrounds, we were able to establish that no significant differences in the produced histomorphometry parameters were seen between imaging in water or in air, suggesting that for biomechanical studies of small isolated specimens in the lab imaging in water is not a necessity for obtaining accurate micro-architectural data.

As limitations we can mention the use of elephant rather than human bone, which is also a mammal but with larger sized bones and consequently the absolute numbers given may not be representative of human tissue. It has however been demonstrated that there is a predictable offset in the structural properties of bone tissue micro-architecture based on the relative sizes of the animals [19] and from these facts possible adjustments can be made to predict what the present data values will be for humans. The samples were also taken from just one animal, so they may lack the interindividual variability that may have been evident otherwise. In an ideal scenario, this study would be repeated using human bone samples taken from various sites around the body and using

multiple individuals representative of both sexes and a range of age groups. The clinical relevance and translation of this work could be further improved in the future by producing and adding HU units values [20]. The imaging resolution was insufficient to explore the vascular micro-architecture, which has been suggested to be in length scale $<1 \mu\text{m}$ [17]. This is also part of the specific surface of bone (sites for cellular activity for bone remodelling), the intracortical porosity of osteonal canals and Volkmann canals within the cortical bone itself, which is in remodelling terms actively porous to a significant extent. As shown by Fig. 5, we have produced BS/TV vs. BV/TV curves that are remarkably similar and consistent with those previously reported by Martin [5]. Small differences at the point where the apex of the curve is (peak) and the actual overall height are to be expected considering possible differences between elephant and human bone and the two different methodologies that have been used.

A comparison of the results throughout all parameters when the scan threshold is placed by using the three backgrounds (air, water, collagen) showed that thresholding at the collagen level has the greatest effect on the morphological results produced from the μCT . This suggests that bone density varies with depth within the bone tissue and that lower density tissue exists nearest to the available surface. It has also been shown that imaging in either water or air does not produce significantly different results; this is an important discovery as it shows that, contrary to what is often recommended, imaging dry or wet bone samples should not have a statistically significant impact on the results. The differences seen between the collagen threshold versus the air and water may suggest that the structure of bone varies with depth from the surface with low density material being more superficial perhaps due to more recent remodelling activity, a fact which we have tried to explore and exploit recently [1]. To a small extent this could also be an artefact from the partial volume effect from μCT imaging; this occurs when the scan voxels at a boundary contain both the sample and the background, which in turn reduces the density of the voxel. This however only happens for just one layer of voxels, those at the edge which contain both bone and its surrounding medium.

270

5. CONCLUSIONS

Setting the most appropriate scanning threshold is critical in producing accurate bone microarchitectural parameters by micro scanning, and we have shown here that values between the different sets of data differed by as much as 85% in some cases. Overall, the values produced for thresholds based on organic material deviated greatly from those based on air and water. We believe that knowing this result is very useful for cases where bone is inspected with this non-

275

destructive imaging method. The relationship between BS/TV vs. BV/TV in particular produced by μ CT scans can be used in the development of models that predict bone remodelling. Developing such models is vitally important in understanding how the skeleton behaves and could lead to further understanding of the underlying mechanism that drives the remodelling process. It could also enable a more profound understanding of the underpinning processes which may help in diagnosis, an earlier identification of abnormal or diseased bone, or those that might be at greater fracture risk.

285 **Acknowledgments**

The tests were carried out in the Biomechanics laboratories of the Cranfield Forensic Institute of Cranfield University in Shrivenham, UK. The authors acknowledge the in-kind support of the Cranfield Forensic Institute and the Department of Comparative Biomedical Sciences (RVC) and ZSL Whipsnade Zoo for provision of the specimen.

290 **Conflict of Interest**

The authors declare that the research was conducted in the absence of any commercial or financial relationships that could be construed as a potential conflict of interest.

Author Contributions

Conceptualization: PZ, RC, GA, JH. Data curation: GA, PZ. Formal analysis: GA, PZ. Funding acquisition: PZ, JH. Investigation: GA, PZ, RC, JH. Methodology: GA, PZ. Project administration: PZ. Resources: PZ, JH. Software: GA. Supervision: PZ, RC, JH. Validation: PZ, RC. Visualization: GA. Writing (original draft): GA, RC. Writing (review and editing): GA, PC, PZ, JH.

Funding

The authors acknowledge the support of the EPSRC (GR/N33225; GR/N33102; GR/ M59167) & BBSRC (BB/C516844/1).

Data accessibility

Data for this manuscript when the article is in print will be available through the Cranfield University CORD data depository and preservation system at <https://cranfield.figshare.com>

Ethical Approval

305 **No HTA approval required**

References

- 310 [1] M Berli, C Borau, O Decco, GJ Adams, RB Cook, JM Garcia Aznar, P Zioupos. Localized tissue mineralization regulated by bone remodelling: A computational approach. PLOS ONE 12(3) (2017) e0173228. doi.org/10.1371/journal.pone.0173228
- [2] GJ Adams, Quality factors at the material and structural level that affect the toughness of human cancellous bone. PhD dissertation, 2017, Cranfield University, UK. <http://dspace.lib.cranfield.ac.uk/handle/1826/15952>
- 315 [3] P Zioupos, RB Cook, JR Hutchinson. Some basic relationships between density values in cancellous and cortical bone. Journal of Biomechanics, 41(9) (2008) 1961-8. doi:10.1016/j.jbiomech.2008.03.025.
- [4] GJ Adams, RB Cook, JR Hutchinson, P Zioupos. Bone Apparent and Material Densities Examined by Cone Beam Computed Tomography and the Archimedes Technique: Comparison of the Two Methods and Their Results. Frontiers in Mechanical Engineering. 3 (2018) doi.org/10.3389/fmech.2017.00023
- 320 [5] RB Martin. Porosity and specific surface of bone. Critical reviews in biomedical engineering, 10(3) (1984) 179-222.
- [6] DP Fyhrie, NL Fazzalari, R Goulet, SA Goldstein. SA. Direct calculation of the surface-to-volume ratio for human cancellous bone. Journal of biomechanics. 26(8) (1993) 955-67. doi.org/10.1016/0021-9290(93)90057-L.
- 325 [7] L J Gibson. The mechanical behaviour of cancellous bone. Journal of Biomechanics, 18(5) (1985) 317-28. doi.org/10.1016/0021-9290(85)90287-8.
- [8] C Greenwood, J Clement, A Dicken, J Evans, I Lyburn, R Martin, K Rogers, N Stone, G Adams, P Zioupos. The micro-architecture of human cancellous bone from fracture neck of femur patients in relation to the structural integrity and fracture toughness of the tissue, Bone Reports, 3 (2015) 67-75. doi: 10.1016/j.bonr.2015.10.001.
- 330 [9] C Greenwood, J Clement, A Dicken, J Evans, I Lyburn, R Martin, K Rogers, N Stone, P Zioupos. Towards new material biomarkers for fracture risk, Bone, 93 (2016) 55-63. doi.org/10.1016/j.bone.2016.09.00. 6.
- 335 [10] C Greenwood, J Clement, A Dicken, J Evans, I Lyburn, R Martin, N Stone, P Zioupos, K Rogers. Age-related changes in femoral head trabecular microarchitecture, Aging and Disease, 9 (6) (2018) 976-87. doi: 10.14336/AD.2018.0124.

- [11] JD Currey, J.D. Bones: Structure and Mechanics, Princeton University Press, (2002) Princeton NJ.
- 340 [12] G Rouhi, W Herzog, L Sudaki, K Firoozbakhsh, M Epstein. Free Surface Density Instead of Volume Fraction in the Bone Remodeling Equation: Theoretical Considerations. *Forma*, 19 (2004) 165-82. doi:10.1016/j.ijengsci.2006.02.001.
- [13] WD Sharpe. Age changes in human bone: an overview. *Bulletin of the New York Academy of Medicine*, 55(8) (1979) 757-73. PMID: 385089; PMCID: PMC1807695.
- 345 [14] PR Buenzli, CD Thomas, JG Clement, P Pivonka. Endocortical bone loss in osteoporosis: the role of bone surface availability. *Int J Numer Method Biomed Eng*. 29(12) (2013) 1307-22. doi.org/10.1002/cnm.2567
- [15] LA Feldkamp, SA Goldstein, AM Parfitt, G Jasion, M Kleerekoper. The direct examination of three-dimensional bone architecture in vitro by computed tomography. *J Bone Miner Res*. 4(1) 350 (1989) 3-11. doi:10.1002/jbmr.5650040103.
- [16] P Zioupos, RB Cook, JR Hutchinson. More thoughts on the relationship between apparent and material densities in bone. *Journal of Biomechanics*. 42(6) (2009) 794-5. doi.org/10.1016/j.jbiomech.2009.01.014.
- [17] Y-B Yan, W Qi, J Wang, LF Liu, EC Teo, Q Tianxia, JJ Ba, W Lei. Relationship between 355 architectural parameters and sample volume of human cancellous bone in micro-CT scanning. *Medical engineering & physics*, 33(6) (2011) 764-9. doi:10.1016/j.medengphy.2011.01.014.
- [18] RB Cook, P Zioupos. The fracture toughness of cancellous bone. *J Biomech*. 42(13) (2009) 2054-60. doi: 10.1016/j.jbiomech.2009.06.001.
- [19] TM Ryan, CN Shaw. Trabecular bone microstructure scales allometrically in the primate 360 humerus and femur. *Proceedings of the Royal Society B: Biological Sciences*, 280(1758) (2013) 20130172. doi:10.1098/rspb.2013.0172
- [20] P Mah, TE Reeves, D McDavid. Deriving Hounsfield Units using grey levels in cone beam computed tomography. *Dentomaxillofacial Radiology* 39(6) (2010) 323-35. doi:10.1259/dmfr/19603304.
- 365 [21] D Ruffoni, P Fratzl, P Roschger, K Klaushofer, R Weinkamer. The bone mineralization density distribution as a fingerprint of the mineralization process. *Bone* 40, (2007) 1308–1319. doi:10.1016/j.bone.2007.01.012

370 **FIGURE CAPTIONS**

Figure 1. Grey level histogram showing: (a) the peaks labelled for air, water, demineralised sample and native sample. The RED line half way between the BLUE ones (peaks) is where the threshold is placed: (b) when air is taken as the background; (c) when water is taken as the background; and (d) when the demineralised sample (organic matter) is taken as the background. It is clear in this illustration that for whole native bone tissue the border line (BL- arrow) for real bone is between the two peaks for water and collagen, that is where water 'ends' and bone tissue (including small amounts of osteoid and epithelial tissue) 'begins'. Unfortunately, in practice and in all cases this trough between water and collagen is never apparent or easy to define, it is buried in the tail end of the water peak. It has only become clear here because we used this technique of demineralising some of the same bone tissue to create a peak for truly native demineralised bone tissue. Notably, to create a noticeable peak a substantial mass of demineralised bone is needed because collagen is much lighter than mineral and less able to absorb x-rays. Importantly, when using the Archimedes technique (immersion and suspension in a medium [2-4]) the actual threshold (red bar) is on the water peak itself (Arch -arrow) where the blue bar is on the water peak in (c).

380
385 Figure 2. (a) QRM Calibration phantom images and histogram (data in Table 1); (b) the resultant calibration curve (using the calibration certificate nominal values) which produces density values from CT grey level (the error bars shown are \pm SD).

Figure 3. Microscope images (backscattered SEM) showing the mosaic of micro-compartments of bone tissue in: (a) cortical bone (cross section of femur, 60 yr old male) and (b) in cancellous bone (modified from Adams et al. [4] and original from Ruffoni et al. [21]). The various tissue compartments are labelled as '1' being the more recent, towards '5' being the older one using the grey level scale whereby the lighter the area the denser it is and the older the tissue age. If the threshold is raised to exclude bone pockets such as '1' the microarchitectural analysis would then apply to the part of bone within the red-dotted area, which becomes then the 'new' bone surface.

395
400 Figure 4. BV/TV and D_{mat} bone material density (g/cm^3) from Archimedes immersion method and from μ CT with 3 different thresholds. (a) BV/TV , water (open red diamonds) and air (blue solid circles) produce similar results, the collagen background (solid green squares) shifts the data significantly downwards, BV/TV from CT is severely eroded when collagen is the threshold and has values between 30-50% smaller than BV/TV by Archimedes especially for intermediate BV/TV values (Black dashed line is line of equality; air: $y = 0.697x + 0.299x^9$, $R^2 = 0.971$; water: $y = 0.687x + 0.314x^9$, $R^2 = 0.971$; collagen: $y = 0.418x + 0.527x^9$, $R^2 = 0.964$); (b) D_{mat} the water threshold produces results

with greater scatter (probably through affecting absorption of the x-rays), the curves for air and collagen are practically identical. For high D_{mat} values (BV/TV near 0 or 1) the CT and Archimedes techniques produce equal values (on average) but for lower density bone samples (intermediate
405 BV/TV) the CT overestimates D_{mat} compared to Archimedes. (Black dashed line is line of equality; air: $y = 0.924 + 0.524 x$, $R^2 = 0.686$; water: $y = 0.453 + 0.756 x$, $R^2 = 0.428$; collagen: $y = 0.951 + 0.510 x$, $R^2 = 0.726$).

Figure 5. Specific surface BS/TV vs. bone volume BV/TV measured using μ CT for all 112 samples from an elephant femur. The samples having $D_{app} > 1.3$ are encircled as this is the BV/TV level
410 beyond which histology would have conventionally defined it as being cortical bone. Black solid parabola is the behaviour of data produced by Martin [5] added here for comparison (similar to Berli et al. [1]).

Figure 6. Specific surface (BS/TV) vs. bone volume (BV/TV) measured using μ CT on 31 samples, those where both mineralised and demineralised bone was present in the scan and in three
415 different background thresholds. Red open diamonds = imaged in water, blue solid circles = imaged in air and green solid squares = with a collagen background. For the remodelling process working through an active surface, relatively more bone tissue volume can be accessed at the intermediate range of BV/TV values, not at the two extremes (cancellous and cortical). The values for BS/TV at its peak derived from the collagen background are 30% less than those derived with respect to water
420 and air backgrounds.

Figure 7. Material density (D_{mat}) vs. BV/TV, by μ CT, for air (blue), water (red) and collagen (green) backgrounds and by using Archimedes immersion method (black). Remodelling working through the available specific surface, according to the model by Berli et al. [1], modulates the mineral content (tissue density) accordingly. All four methods indicate that in mid-range BV/TV the
425 organic content is relatively higher and the tissue density lower as a result. The values of D_{mat} at the trough are higher by 32% for water, 68% for air and 84% for collagen as backgrounds with respect to the $D_{mat} / (BV/TV)$ behaviour derived by the Archimedes method. (Archimedes: $D = 2.02 - 0.977 (BV/TV) + 0.749 (BV/TV)^3 + 0.303 (BV/TV)^9$, $R^2 = 0.767$; air: $D = 1.93 - 0.450 (BV/TV) + 0.675 (BV/TV)^2 - 0.151 (BV/TV)^9$, $R^2 = 0.734$; water: $D = 1.88 - 0.332 (BV/TV) + 0.519 (BV/TV)^3$, $R^2 = 0.446$; collagen: $D = 1.83 + 0.196 (BV/TV) + 0.054 c(BV/TV)^3$, $R^2 = 0.496$).

Figure 8. (a) BS/BV vs. BV/TV for the full range of 112 samples and (b) for the sub-group of 31 samples measured with different backgrounds: Red open diamonds = in water, blue solid circles = in air and green solid squares = with a collagen background. The values for BS/TV from collagen
backgrounds across the BV/TV range are lower by 25% to 30% with respect to the values produced

435 with air and water backgrounds. Naturally in the absence of any pores and voids the absolute limit
for BS/BV is zero as BV/TV tends to 1. It is a simple corollary of geometry and morphometrics that
the specific surface area (area over the enclosed volume) of a particle tends towards very high
values for any geometrical scheme regardless if it is bone or anything else (the finer the power the
highest specific surface area; $\text{Area/Volume} = f(R^2)/f(R^3) \sim 1/R$ with R approaching zero the value
440 approaches infinity).

Figure 9. (a) Trabecular thickness (TbTh) vs. BV/TV for the full range of 112 samples and (b)
for the sub-group of 31 samples measured with different backgrounds: Red open diamonds = in
water, blue solid circles = in air and green solid squares = with a collagen background. The values for
TbTh produced from collagen background are between 40% and 85% higher than the ones produced
445 on air and water backgrounds.

Figure 10. (a) Trabecular spacing (TbSp) vs. BV/TV for the full range of 112 samples and (b) for
the sub-group of 31 samples measured with different backgrounds: Red open diamonds = in water,
blue solid circles = in air and green solid squares = with a collagen background. The values for TbSp
are lower at the higher end of BV/TV values for collagen background by up to 85% comparing to air
450 and water backgrounds.

Revised MS with tracked changes

Author Contributions

Conceptualization: PZ, RC, GA, JH. Data curation: GA, PZ. Formal analysis: GA, PZ. Funding acquisition: PZ, JH. Investigation: GA, PZ, RC, JH. Methodology: GA, PZ. Project administration: PZ. Resources: PZ, JH. Software: GA. Supervision: PZ, RC, JH. Validation: PZ, RC. Visualization: GA. Writing (original draft): GA, RC. Writing (review and editing): GA, PC, PZ, JH.